proceedings

MDPI

Proceedings

Comparison of the Performances of Two Aptamers on a Colorimetric Assay for the Quantification of Fumonisin B1 †

Vicente Antonio Mirón-Mérida *, Yadira González-Espinosa, Yun Yun Gong, Yuan Guo and Francisco M. Goycoolea *

School of Food Science and Nutrition, University of Leeds, Leeds LS2 9JT, UK;
Y.GonzalezEspinosa@leeds.ac.uk (Y.G.-E.); Y.Gong@leeds.ac.uk (Y.Y.G.); Y.Guo@leeds.ac.uk (Y.G.)

* Correspondence: fsvamm@leeds.ac.uk (V.A.M.-M.); F.M.Goycoolea@leeds.ac.uk (F.M.G.)

† Presented at the 1st International Electronic Conference on Biosensors, 2–17 November 2020; Available online: https://iecb2020.sciforum.net/.

Published: 2 November 2020

Abstract: Fumonisin B1 (FB1), a mycotoxin commonly produced by *Fusarium verticillioides* and classified as a group 2B hazard, has been identified in various food products; hence, sensitive and rapid analytical detection methods are needed. Since the first reported aptamer (96 nt ssDNA) for the highly specific molecular recognition of FB1, only 30 aptamer-based biosensors have been published. A critical point, yet commonly overlooked during the design of aptasensors, is the selection of the binding buffer. In this work, a colorimetric assay was designed by incubating a folded aptamer with FB1 and the subsequent addition of gold nanoparticles (AuNPs). The changes in the aggregation profile of AuNPs by a 40 nt aptamer and a 96 nt aptamer were tested after the addition of FB1 under different buffer conditions, where the incubation with Tris-HCl and $MgCl_2$ exhibited the most favorable performances. The assay with the longest aptamer was specific to FB1 and comparable to other aptasensors with a limit of detection (LOD) of 3 ng/mL ($A_{650/520}$ ratio). Additionally, the application of asymmetric-flow field-flow fractionation (AF4) with multidetection allowed for the analysis of the peak area (λ) and multi-angle light scattering (MALS) with LODs of up to the fg/mL level.

Keywords: Fumonisin B1; gold nanoparticles; aptamer; AF4

1. Introduction

Fumosinin refers to a family of mycotoxins from which group B is the most abundant in nature [1]. From this group, fumonisin B1 (FB1) ($C_{34}H_{59}NO_{15}$) has been monitored in multiple food commodities due to the fact of its harmful effects on animals and classification as a possible carcinogenic to humans [2]. Conventional methods for mycotoxin detection include ELISA, HPLC-FLD, and LC-MS, and they implicate high costs, long assays, poor portability, and experienced analysts [3]. Hence, sensitive, quick, and affordable methods should be developed for the quantification of mycotoxins.

An alternative to the traditional methods is the integration of biosensing techniques with aptamers, single-stranded DNA or RNA molecules with high affinity to specific target molecules. The SELEX selection of specific aptamers for FB1 has resulted in the discovery of two main sequences, namely, 96 nt and 80 nt. Both sequences are already employed in approximately 30 aptasensors [4,5], where a critical step during their engineering is the selection of the optimum target–aptamer incubation conditions (i.e., buffer, incubation, temperature).

Gold nanoparticles (AuNP), widely utilized in multiple biosensing platforms, can be functionalized with aptamers for the colorimetric detection of FB1. This approach relies on the aggregation of AuNPs in the presence of cationic compounds [6,7]. Besides spectrophotometric analysis of AuNPs, asymmetric-flow field-flow fractionation (AF4) with multidetection (refractive index (RI), multi-angle light scattering (MALS), dynamic light scattering (DLS), and UV-Vis) is a promising technique for the analysis of their interaction with aptamers during target incubation. The AF4 fractionates macromolecules and particles depending on their hydrodynamic radius and, subsequently, determines their distribution based on their concentration, composition, and size using the signals from the different detectors. Such separation occurs due to the parabolic laminar flow passing through a thin membrane, where AuNPs are grouped by a perpendicular flow [8]. In this work, the quantification of FB1 was assessed for two aptamers under different buffer conditions. We gained further insight into the interactions at play between the aptamer–target complex and AuNPs under aggregation conditions (salt addition) using AF4 while harnessing its capacity to fractionate and characterize colloidal particles and biomacromolecules.

2. Materials and Methods

2.1. Colorimetric Determination of FB1 by Functionalization of AuNP with Aptamers

Two aptamers (40 and 96 nt) reported as specific for FB1 were individually incubated with FB1 at different concentrations (the incubation time, temperature, and binding buffers will be specified for each figure), followed by the incubation with AuNP. From this mixture, 30 µL were combined with NaCl in a 1:1 (*v*:*v*) ratio for a wavelength scan (400–800 nm) using a TECAN (Crailsheim, Germany) microtiter plate reader. The A520/650 ratio was determined by dividing the absorbance values at 520 and 650 nm. The general procedure is outlined in Figure 1.

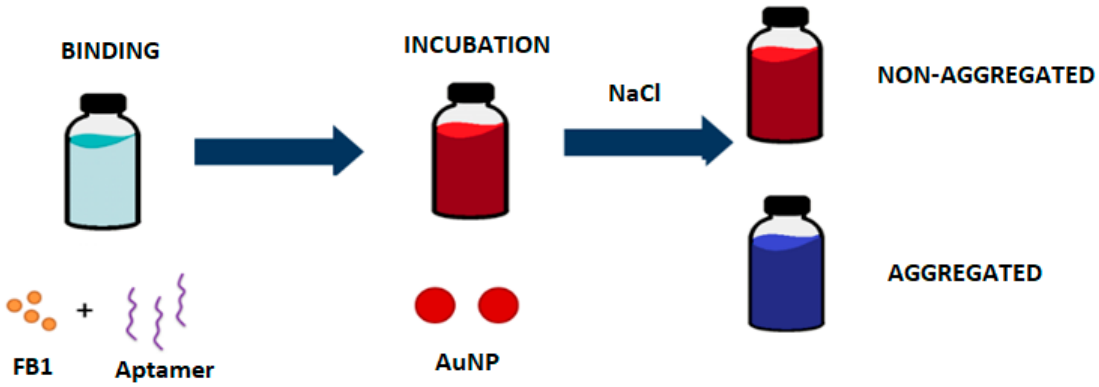

Figure 1. Colorimetric determination of fumonisin B1 (FB1) with gold nanoparticles (AuNPs)–aptamers in bulk.

2.2. Analysis of the AuNP–FB1–Aptamer Complex by Asymmetric-Flow Field-Flow Fractionation (AF4)

Asymmetric-flow field-flow fractionation measurements were performed on an AF2000 Multiflow system from Postnova Analytics GmbH (Landsberg am Lech, Germany). A method for the size separation of AuNPs was developed using a regenerated cellulose membrane with water/surfactant as carrier solvent. The optimized AF4 method consisting in an exponential decay (70 min, cross flow: 1 mL/min, focus pump: 1.30 mL/min) was applied on the aggregation profile of AuNPs stabilized with a FB1–aptamer complex unveiled upon addition of NaCl 0.2 M. The observed characteristic results at different FB1 concentrations were analyzed by UV-Vis (600 nm) and MALS (28°), and the peak area was calculated in Origin Pro 8.6 32 Bit (2012) software, considering the base line of each curve. This provided a new quantification for mycotoxins as well as an alternative method for characterizing aptamer–target interactions.

3. Results and Discussion

3.1. Quantification of FB1 with a 40 nt Aptamer

The values of the $A_{520/650}$ ratio upon incubation of a 40 nt aptamer with varying concentrations of FB1 in Tris-HCl 31.1 mM (pH 7.5), PBS buffer 12.79 mM (pH 7.4), and a combination of both buffer media is illustrated in Figure 2. As it can be noted, an opposite and more differentiated performance was obtained when Tris-HCl buffer was included during the binding step, which was also confirmed by the similarity of both curves containing Tris-HCl buffer. The utilization of Tris-based buffers (pH 8.2) has been tested for diluting FB1 during the incubation with this 40-nt sequence at 37 °C as part of the electrochemical detection with graphene-modified electrodes [9,10].

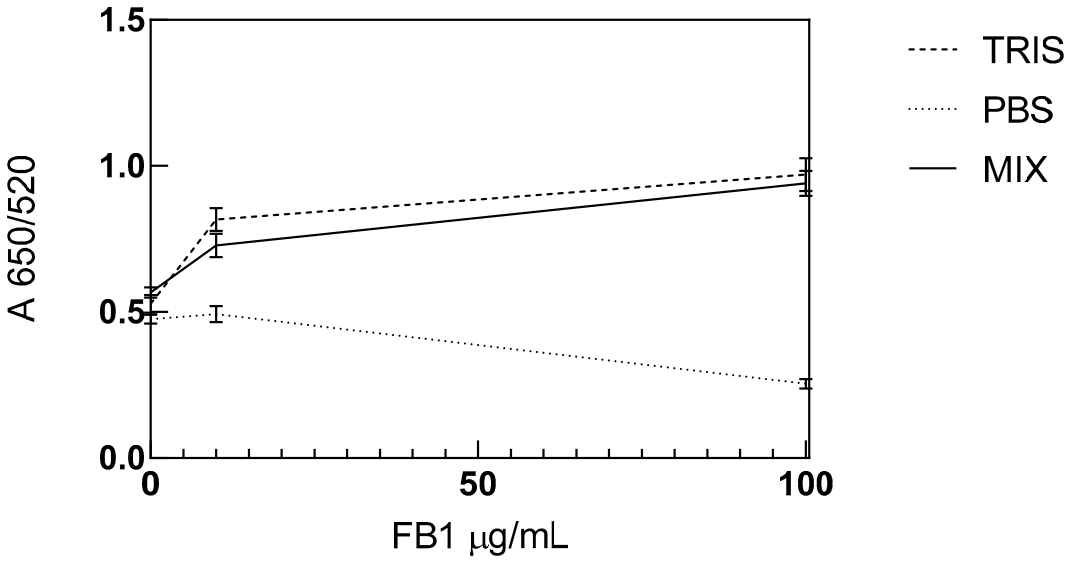

Figure 2. Effect of the incubation in Tris-HCl (31.1 mM, pH 7.5), PBS buffer (12.79 mM, pH 7.4), and both buffer media (MIX) on the functionalization effect of a 40-nt aptamer on AuNPs at increasing FB1 concentrations upon the addition of NaCl 0.4 M (aptamer–FB1 binding: 60 min at 37 °C; AuNP incubation: 120 min at 37 °C; 117:1 aptamer:AuNP molar ratio).

As shown in Figure 3a, the incubation of aptamers (40-nt) and FB1 in Tris-HCl buffer resulted in a favorable sensing resolution with a limit of detection equivalent to 30 ng/mL Nevertheless, such a biosensing approach was not specific for FB1 (Figure 3b), as incubation with the same concentration of ochratoxin A (OTA) resulted in a similar $A_{650/520}$ ratio to that of FB1. This result is contrary to the previously reported specificity for an electrochemical method integrating the same aptamer that has an affinity to FB1, which was confirmed through specificity assays with OTA and thrombin [10].

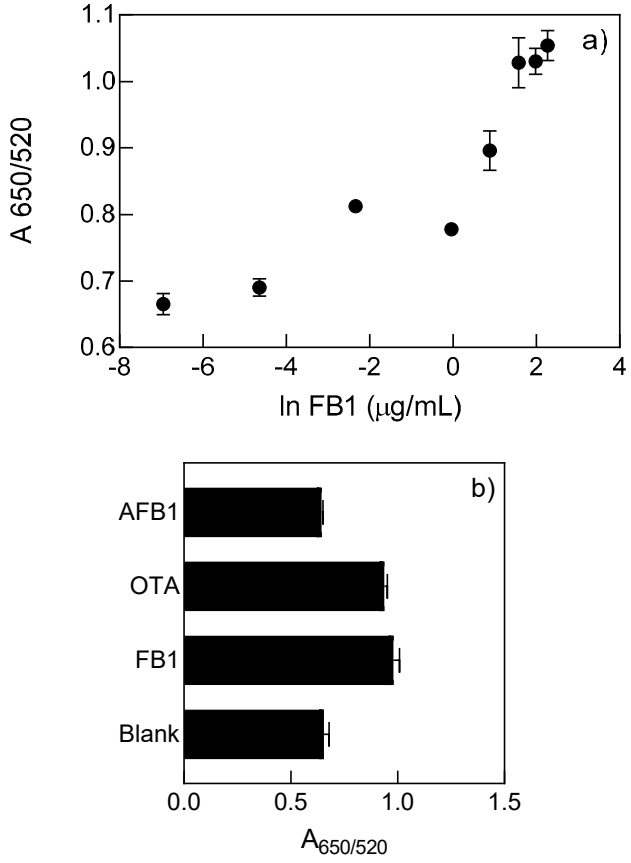

Figure 3. The $A_{650/520}$ ratio of AuNPs functionalized with a 40-nt aptamer previously incubated with FB1 in Tris-HCl 14.06 mM pH 7.5 (incubation: 60 min at 37 °C, functionalization: 105 min at 20 °C, aptamer:AuNP 117:1) after the addition of NaCl 0.4 M (**a**); specificity test after the incubation with a buffer (blank), FB1, aflatoxin B1 (AFB1), and ochratoxin A(OTA) at a mycotoxin concentration of 13.8 μM (**b**).

3.2. Quantification of FB1 with a 96 nt Aptamer

The first sequence reported for FB1 [4] was utilized in this work for the development of a colorimetric technique by completing the steps outlined in Figure 1. Despite the attempts to produce a noticeable signal at low FB1 concentrations, neither PBS nor Tris-HCl were successfully applied on the establishment of an aptamer-based sensing strategy. However, as displayed in Figure 4a, MgCl2 was confirmed as an optimal buffer for a more sensitive determination of FB1, where the limit of detection based on the $A_{650/520}$ ratio was calculated as ~3 ng/mL. The protective effect of the aptamer–FB1 complex on the surface of AuNPs was specific for the target mycotoxin, as demonstrated in Figure 4b, where similar aggregation profiles were found among OTA, AFB1, and the blank sample. The reduction in the aggregation of AuNPs by their stabilization with an aptamer–target complex has been explored in other molecules, such as serotonin, where the binding buffer prevents the repulsion among the DNA backbone negative charges, for an improved folding and complex formation [11].

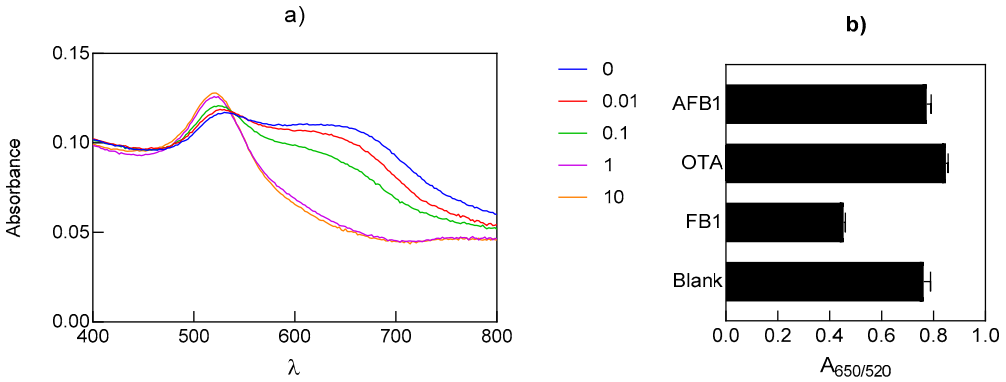

Figure 4. The UV-Vis spectra of AuNPs functionalized with a 96-nt aptamer previously incubated with FB1 (0–10 µg/mL) in MgCl2 1 mM (binding: 30 min at 37 °C; functionalization: 60 min at RT, aptamer: AuNP 30:1) after the addition of NaCl 0.2 M (**a**); specificity test after the incubation with buffer (blank) or FB1, aflatoxin B1 (AFB1), and ochratoxin A(OTA) at a concentration of 1.38 µM (**b**).

3.3. Analysis of AuNPs functionalized with an Aptamer–FB1 complex by Asymmetric-Flow Field-Flow Fractionation (AF4)

Unlike other aptasensors in which the addition of the target molecule promotes the whole DNA sequence detachment from AuNP or its dehybridization from complementary sequences, this biosensor presents the formation of an Aptamer–FB1–AuNP complex that is more stable to particle aggregation (NaCl 0.2 M) at higher FB1 concentrations.

As displayed in Figure 5a, the movement of particles through the membrane occurred from a smaller to greater size, which in the case of the aptamer–FB1–AuNP conjugate can be translated into non-aggregated to aggregated particles. Therefore, higher peaks were observed by the end of each run, where a larger size and more aggregated particles were expected, especially at 600 nm, where the aggregation profile was more notorious by UV-Vis. After calculating the area under the highest peak (from 20 min run), the limit of detection was estimated as 0.000056 ng/mL (56 fg/mL). Similarly, the MALS results at 28° (Figure 5b) indicated a single predominant peak towards the end of each run, with a reduction in the peak height at increasing FB1 concentrations. This signal also reported a good sensitivity with an LOD of 0.00016 ng/mL. Note that these results are consistent with the notion that the conjugation is promoted by the presence of the target mycotoxin, which was visually confirmed by its red color and now evidenced by the distribution of the different signals in AF4.

These results imply that the main role of FB1 in promoting the functionalization of AuNPs involves the whole aptamer sequence and is not only mediated through its affinity to the molecule, but also by the interaction with the rest of the DNA sequence which is not involved in binding the FB1 epitope region.

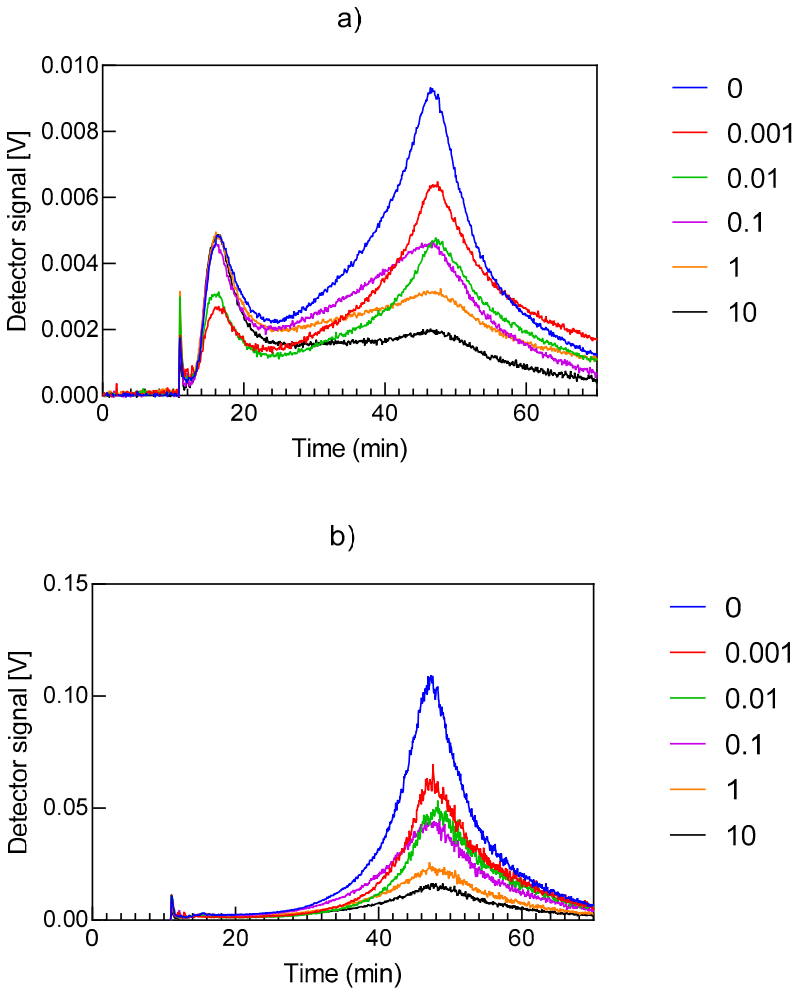

Figure 5. The aptamer–FB1–AuNP conjugate at different FB1 concentrations upon the addition of NaCl (0.2 M) detected by UV: 600 nm (**a**); and MALS: 28° (**b**) signals.

4. Conclusions

In this work, a bulk aptasensor method was developed by incubating an aptamer with its target molecule (FB1) and afterwards with AuNPs. The appropriate incubation conditions (i.e., time, temperature, buffer) derived by the formation of an aptamer–FB1–AuNP conjugate, mediated by the presence of FB1.

Even when acceptable limits of detection were found by analyzing the $A_{650/520}$ ratio from spectrophotometric scans, the analysis of the interaction within the conjugation elements by AF4 revealed a novel potential biosensing technique with a limit of detection in the fg/mL range, with the added novelty of utilizing an ssDNA aptamer sequence without the aid of any complementary strand.

Author Contributions: Conceptualization, V.A.M.-M.; Y.G.; Y.Y.G. and F.M.G.; methodology, V.A.M.-M. and Y.G.-E.; software, V.A.M.-M. and Y.G.-E.; validation, V.A.M.-M.; formal analysis, V.A.M.-M.; investigation, V.A.M.-M.; resources, Y.G., Y.Y.G. and F.M.G.; data curation, V.A.M.-M.; writing—original draft preparation, V.A.M.-M.; writing—review and editing, V.A.M.-M. and F.M.G.; visualization, V.A.M.-M.; supervision Y.Y.G. and F.M.G.; project administration, V.A.M.-M. and F.M.G.; funding acquisition, V.A.M.-M. and F.M.G. All authors have read and agreed to the published version of the manuscript.

Acknowledgments: V.A.M.-M was awarded with a scholarship from CONACyT (Mexico) for his PhD studies.

Conflicts of Interest: The authors declare no conflict of interest.

References

1. Rheeder, J.P.; Marasas, W.F.; Vismer, H.F. Production of fumonisin analogs by Fusarium species. *Appl. Environ. Microbiol.* **2002**, *68*, 2101–2105.
2. Ostry, V.; Malir, F.; Toman, J.; Grosse, Y. Mycotoxins as human carcinogens—The IARC Monographs classification. *Mycotoxin Res.* **2017**, *33*, 65–73.
3. Lee, S.; Kim, G.; Moon, J. Performance improvement of the one-dot lateral flow immunoassay for aflatoxin B1 by using a smartphone-based reading system. *Sensors* **2013**, *13*, 5109–5116.
4. McKeague, M.; Bradley, C.R.; Girolamo, A.D.; Visconti, A.; Miller, J.D.; DeRosa, M.C. Screening and initial binding assessment of Fumonisin B1 aptamers. *Int. J. Mol. Sci.* **2010**, *11*, 4864–4881.
5. Chen, X.; Huang, Y.; Duan, N.; Wu, S.; Xia, Y.; Ma, X.; Zhu, C.; Jiang, Y.; Ding, Z.; Wang, Z. Selection and characterization of single stranded DNA aptamers recognizing fumonisin B1. *Microchim. Acta* **2014**, *181*, 1317–1324.
6. Pandey, P.C.; Pandey, G. Synthesis of gold nanoparticles resistant to pH and salt for biomedical applications; functional activity of organic amine. *J. Mater. Res.* **2016**. *31*, 3313-3323.
7. Rosi, N.L.; Mirkin, C.A. Nanostructure in biodiagnostics. *Chem. Rev.* **2005**, *105*, 1547–1562.
8. Hagendorfer, H.; Kaegi, R.; Traber, J.; Mertens, S.F.L.; Scherrers, R.; Ludwig, C.; Ulrich, A. Application of an asymmetric flow field flow fractionation multi-detector approach for metallic engineered nanoparticle characterization- Prospects and limitations demonstrated on Au nanoparticles. *Anal. Chim. Acta* **2011**, *706*, 367–378.
9. Tian, H.; Sofer, Z.; Pumera, M.; Bonanni, A. Investigation on the ability of heteroatom-doped graphene for biorecognition. *Nanoscale* **2017**, *9*, 3530–3536.
10. Cheng, Z.X.; Bonanni, A. All-in-One: Electroactive Nanocarbon as Simultaneous Platform and Label for Single-Step Biosensing. *Chem. Eur. J.* **2018**, *24*, 6380–6385.
11. Chávez, J.L.; Hagen, J.A.; Kelley-Loughnane, N. Fast and selective plasmonic serotonin detection with aptamer-gold nanoparticle conjugates. *Sensors* **2017**, *17*, 681.